FPGA Implementation of a Probabilistic Neural Network Using Delta-Sigma Modulation for Pattern Discrimination of EMG Signals

Keisuke Shima, and Toshio Tsuji
Graduate School of Engineering, Hiroshima University
Higashi-Hiroshima, Japan 739-8527
Email: {keisuke, tsuji}@bsys.hiroshima-u.ac.jp

***Abstract*— This paper proposes a novel probabilistic neural network (PNN) using delta-sigma modulation (DS modulation) with the aim of realizing high performance in the case of the pattern discrimination of bioelectric signals. The proposed network includes a statistical model so that the posterior probability for the given input patterns can be estimated. Moreover, the calculation speed of the proposed network in the hardware can be increased since the 1-bit pulse signals with delta-sigma modulators (DSMs) are used for the realization of the internal calculation of the network. In this paper, we implemented the proposed network on a field programmable gate array (FPGA), and discrimination experiments were conducted using the artificial data and the electromyogram (EMG) patterns of an amputee. In the experiments, we confirmed that the proposed network has a high accuracy of pattern discrimination.**

I. Introduction

Probabilistic neural networks (PNNs) can be used to solve statistical pattern recognition problems based on the Bayesian discrimination theorem, wherein a probability model is introduced into the network structure to estimate the posterior probability for given input patterns by appropriately training the synaptic weights [1]. Because the PNNs can atain high accuracy in the problems of pattern discrimination, they have been applied to the pattern discrimination problems for bioelectric signals such as electroencephalograms (EEGs) and electromyograms (EMGs) [1]–[3].

Bioelectric signals such as EMGs reflect the internal conditions of the human body and the intention regarding body motions. If the motion intention can be estimated from biological signals, it could be used as a control signal for artificial limbs and human-machine interfaces. Our research group proposed a PNN for the pattern discrimination of bioelectric signals, which is called a log-linearized Gaussian mixture network (LLGMN) [3]. The LLGMN estimates the posterior probability based on the Gaussian mixture model (GMM) and the log-linear model, and it results considerably high ability in the case of EEG and EMG pattern discrimination problems. Then, the LLGMN has been used to develop various human-machine interface for myoelectric prosthetic hands, an EMG-based pointing device, and an EMG-controlled electric wheelchair [4]–[7]. In such systems, the software implementation of the LLGMN on a general-purpose computer was adopted; however, the development of practical human interface applications was difficult because the implementation of the interface devices to be compact and portable as much as possible was quite essential.

On the other hand, various neural networks (NNs) have been implemented in digital hardware [8], [9]. Generally, hardware implementations are achieved based on application specific integrated circuit (ASIC) and field programmable gate array (FPGA) devices. We also implemented the LLGMN on an FPGA chip and verified it on an EMG-based pointing system [5]. However, the digital circuit scale in [5] was very large because it adopted multiple bits representation of variables used in the LLGMN. Moreover, it could not fully utilize the ability of parallel processing in the digital hardware since the LLGMN is not structurally compatible with the hardware architecture in the network.

Generally, every FPGA has the limitation of the digital circuit scale. In order to cope with this problem, pulsed NNs have been widely applied to realize the parallel processing in NNs [10]–[12]. Recently, these networks have received considerable attention since internal neurons are connected by a single wire; therefore, a larger number of neurons can be implemented in parallel. Further, pulsed NNs are expected to reduce the digital circuit scale during implementation since the internal arithmetic is calculated using 1-bit pulse signals. In particular, Murahashi *et al*. [11] proposed a pulsed NN model, which used delta-sigma modulation (DS modulation) as the 1-bit pulse signal generation method, and some learning algorithms such as generalized harmonic analysis (GHA) and back-propagation (BP) learning were realized. However, because bioelectric signals such as EMGs are greatly influenced by individual differences, it is preferable to use PNNs as the pattern discrimination method. Because these networks can estimate the probability density function (pdf) from small sample size data, they can discriminate on the basis of the statistical model.

In this paper, for the aim of introducing hardware architecture and statistical models into the NN, we propose a novel PNN that combines a pulsed NN with the LLGMN. Since DS modulation is used as the 1-bit pulse signal generation method and the elemental device of the internal calculations, the circuit scale of the PNN in hardware could be reduced. In addition, regarding the statistical pattern discrimination of

1-4244-1078-9/07/$25.00

bioelectric signals, the realized NN hardware can be expected to exhibit high performance.

This paper is organized as follows. Section II explains the architecture and algorithm of the PNN using DS modulation. The discrimination experiments for the artificial data are presented in section III, and the feature extraction and discrimination algorithm of EMG signals are presented in section IV. The final section gives the conclusion of this paper.

II. Probabilistic neural network using delta-sigma modulation

In the proposed PNN, DS modulation, which is a type of 1-bit pulse modulation method, is used as the realization method for the internal arithmetic of the LLGMN proposed by Tsuji *et al*. [3]. In the following subsections, the internal architecture of the LLGMN is shown and the proposed calculation method for the LLGMN using DS modulation is explained.

A. LLGMN [3]

The LLGMN is based on the GMM and the log-linear model of the pdf. By applying the log-linear model to a product of the mixture coefficients and the mixture components of the GMM, a semiparametric model of the pdf is incorporated into a three-layer feed-forward PNN. Through learning, the LLGMN distinguishes the signal patterns with individual differences and the lag in its measurement, thereby enabling precise pattern recognition for bioelectric signals [3]–[7]. In this subsection, the internal architecture and algorithm of the LLGMN is presented.

The structure of LLGMN is shown in Fig. 1. First, the input vector $\boldsymbol{x} \in \Re^d$ is converted into the modified vector $\boldsymbol{X} \in \Re^H$ as follows:

$$\begin{aligned}\boldsymbol{X} \;&=\; [1, \boldsymbol{x}^{\mathrm{T}}, {x_1}^2, x_1x_2, \cdots, x_1x_L, x_2^2, x_2x_3, \\ &\quad\; \cdots, x_2x_L, \cdots, {x_L}^2]^{\mathrm{T}} \end{aligned} \tag{1}$$

where $x_i, i = 1, 2, \ldots, d$, are the elements of $\boldsymbol{x}$ and $H = 1 + L(L+3)/2$. The first layer consists of H units corresponding to the dimension of $\boldsymbol{X}$ and the identity function is used for activation of each unit.

In the second layer, each unit receives the output of the first layer weighted by the weight $w_h^{(k,m)}$ $(h = 1, 2, \ldots, H; k = 1, \ldots, K; m = 1, \ldots, M_k)$ and outputs the posterior probability of each Gaussian component. Here, K denotes the number of classes, and M_k is the number of Gaussian components in class k. The relationships between the input of unit $\{k, m\}$ in the second layer ${}^{(2)}I_{k,m}$ and the output ${}^{(2)}O_{k,m}$ are defined as

$${}^{(2)}I_{k,m} = \sum_{h=1}^{H} {}^{(1)}O_h w_h^{(k,m)} \tag{2}$$

$${}^{(2)}O_{k,m} = \frac{\exp[{}^{(2)}I_{k,m}]}{\displaystyle\sum_{k'=1}^{K} \sum_{m'=1}^{M_{k'}} \exp[{}^{(2)}I_{k',m'}]} \tag{3}$$

where $w_h^{(K,M_k)} = 0$ $(h = 1, \ldots, H)$.

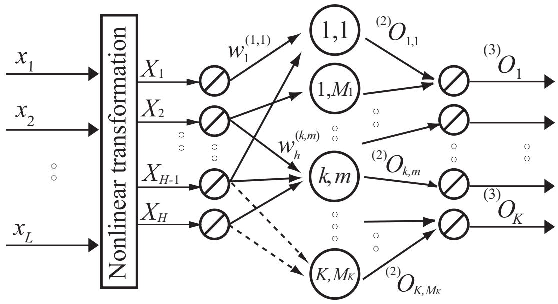

Fig. 1. Structure of the LLGMN [3].

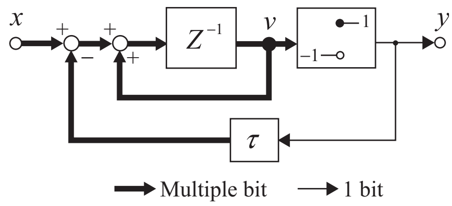

Fig. 2. Delta-sigma modulator [11].

The third layer consists of K units corresponding to the number of classes. The unit k sums up the outputs of M_k components k, m in the second layer. The function between the input and the output is described as

$${}^{(3)}O_k = {}^{(3)}I_k = \sum_{m=1}^{M_k} {}^{(2)}O_{k,m} \tag{4}$$

where the output ${}^{(3)}O_k$ corresponds to the posterior probability of class k.

B. Delta-sigma modulation and neural network model

1) DS modulation [11]: DS modulation is a technique in which the input signal such as multi-bit signals and analog signals is converted into a 1-bit pulse signal, and it has been attracting interests in various fields such as acoustics and communications. The distinctive feature of DS modulation is that the SN ratio is improved when the sampling frequency is increased much higher than the frequency required for the original signal; because the quantization noise in the output of the delta-sigma modulator (DSM) is generated in the high-frequency band, the quantization noise can be reduced in the original signal which exists in the low-frequency band. The structure of a bipolar-type DSM is shown in Fig. 2, where the output takes the values "-1" and "$+1$. " In this figure, the bold line represents multi-bit signals and the thin line 1-bit signals. The output y of the circuit can be expressed in the form of

$$v = \frac{z^{-1}}{1 - z^{-1}} \{x - \tau y\} \tag{5}$$

$$y = \begin{cases} 1 & (v \geq 0) \\ -1 & (v < 0) \end{cases} \tag{6}$$

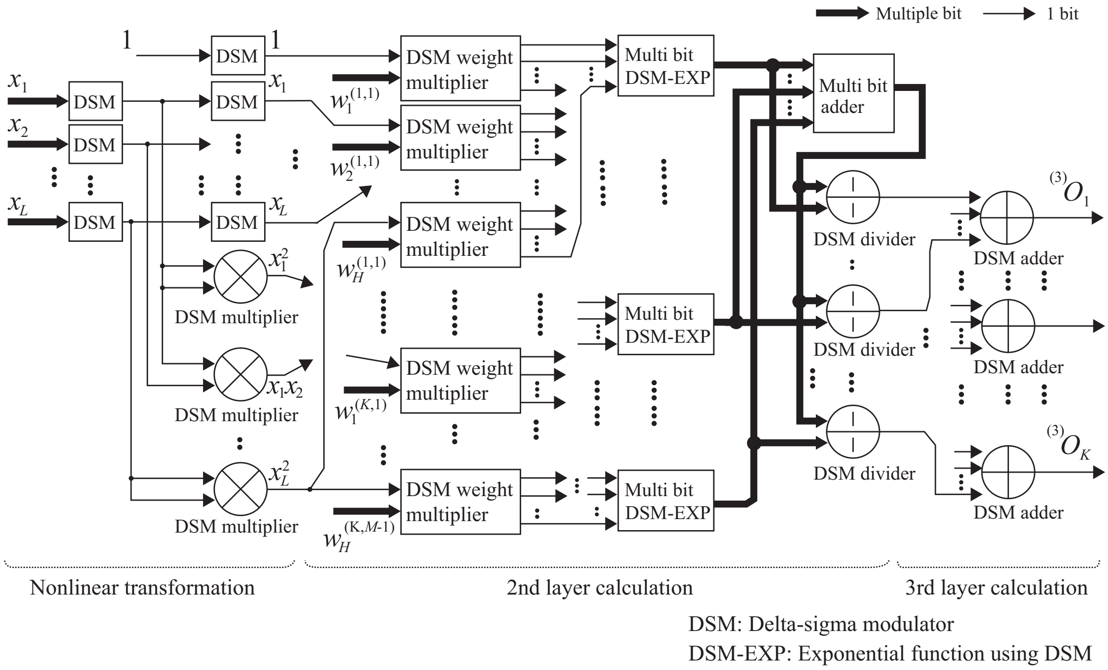

Fig. 3. Structure of an LLGMN based on DS modulation.

where x is the input, v is the integrated value of the quantization error, and $\tau > 0$ is the feedback gain. Here, "-1" and "$+1$" are represented by the low level and the high level in the hardware, respectively. Since the feedback is sent from the output to the input, the quantization errors become virtually equal to 0 and thus the output signal is almost the same as the input signals [12].

The generated 1-bit pulse signal can be easily demodulated using a low-path filter. Then, Murahashi *et al*. [11] proposed the unified signal processing algorithms such as 1-bit adders and multipliers. This paper describes the realization method of the internal calculation of the LLGMN using DSMs and the signal processing algorithms proposed by Murahashi *et al*. [11].

2) LLGMN using DSMs: The pulsed NNs using 1-bit signals can prevent the circuit scale from increasing. The calculable ranges of the NNs, however, are limited to the range from -1 to $+1$. The weight coefficients of the LLGMN can be any real number and exponential functions are used in the second layer as output functions of the LLGMN. Therefore, the internal calculation of the LLGMN involves a high degree of risk that cannot be calculated from -1 to $+1$ by DSM. The restrictions of the calculation range are necessary for realizing the internal calculation of the LLGMN using DSMs.

The proposed structure of the LLGMN based on DS modulation is shown in Fig. 3. The network consists of 1-bit adders, 1-bit multipliers, weight multipliers using DSM, and so on. Here, the input data are normalized to its minimum value of -1 and maximum value of $+1$ as a prerequisite for pattern discrimination.

First, the input data are converted from multi-bit signals to 1-bit signals using DSMs and nonlinearly transformed using the $(H - L - 1)$ 1-bit multipliers. Next, for the calculation of the weight coefficients, the input function of the second layer is converted as follows:

$$^{(2)}I_{k,m} = \sum_{h=1}^{H} \sum_{n=1}^{N} {}^{(1)}O_h \frac{w_h^{(k,m)}}{N} \tag{7}$$

where N is an arbitrary positive integer. It should be noted that the value of each term in the right-hand side of this equation can be restricted to the range from -1 to $+1$ if N is appropriately set according to the value of the weight coefficients. Further, the exponential function included in the LLGMN can be approximated as follows by using the Taylor series [13]:

$$\begin{aligned} \exp[^{(2)}I_{k,m}] &= \prod_{h=1}^{H} \prod_{n=1}^{N} \exp\left[{}^{(1)}O_h \frac{w_h^{(k,m)}}{N} \right] \\ &\cong \prod_{h=1}^{H} \prod_{n=1}^{N} \left[\sum_{c=0}^{C} \frac{1}{c!} ({}^{(1)}O_h \frac{w_h^{(k,m)}}{N})^c \right] \end{aligned} \tag{8}$$

where C is the order of the Taylor series ignoring the high-order terms greater than $C + 1$. Because the range of the values for the input functions of the second layer (see (7)) are restricted between -1 and $+1$, the right-hand side of (8) can be calculated in a range of values between -1 and $+1$.

The output function (3) in the second layer is then realized by using multipliers and dividers, after it is demodulated to multi-bit signals using (8) and low-path filters. Finally, the outputs of the network are calculated by (4) by using the 1-bit adder from the outputs in the second layer. Thus, the posterior probabilities of input patterns can be calculated using DSMs.

Consequently, the posterior probability for given input patterns can be estimated using the DS modulation. The proposed network can discriminate based on the GMM model since the network can take the class with the highest posterior probability as the result of discrimination. Then, the proposed method can be realized as the hardware with the discrimination ability of the LLGMN for bioelectric signals.

III. Numerical experiments

The proposed network realizes all the internal calculations of the LLGMN using DSMs; however, this method has a high risk of reducing the discrimination ability because the internal calculations in this network result some errors such as the 1-bit modulation of input signals and the approximated exponential functions. Then, in order to verify the validity of the proposed PNN, pattern discrimination experiments on artificial data (see Fig. 4) were conducted.

There are two classes ($K = 2$) in a two-dimensional input space; each consists of two Gaussian sources ($M_k = 2$). The centers of the Gaussian distributions in Class one are $(0.35, 0.35)$ and $(-0.35, -0.35)$ and those in Class two are $(0.35, -0.35)$ and $(-0.35, 0.35)$. Further, all the centers have the same variances of 0.0225. The samples from the two classes are represented by $\circ$ and $\times$, respectively, in Fig. 4. The theoretical limit of the error probability for the test dataset is 2.00 [%].

The proposed PNN was implemented on a development board (XtremeDSP Development Kit-II, Nallatech) hosting a Xilinx Virtex family FPGA chip (XCV3000-4FG676). The network is described using Verilog-HDL with ISE 7.1i (Xilinx) design tools and ModelSim XE III 6.0a (Xilinx) as the circuit simulator. The operation frequency of the FPGA is 25 MHz, and the width in bits is 16 for the multi-bit signal. Also, the number of terms in the calculation with the weight coefficient (7) is $N = 25$ and the order of the Taylor series is $C = 4$. With regard to this, the posterior probabilities of two classes are calculated after the 1-bit pulse signals from the output function in the third layer are demodulated to the corresponding multi-bit signals using low-path filters.

The discrimination rates of (1) the software implementation of the multi-layer perceptron (MLP) using C language, (2) the software implementation of the LLGMN, (3) the hardware implementation of the LLGMN [5], and (4) the proposed hardware implementation of the LLGMN using DSMs are shown in Table I. In the experiments, 4000 samples are used as the discrimination data. Because the MLP requires sufficient learning and discrimination abilities, we determined the structure of the MLP based on [3], where the number of layers is 4 and the numbers of neurons in the input layer, hidden layers, and output layer are 2, 10, and 2, respectively. Further, the back-propagation method is used as the learning algorithm. From the table, it can be seen that the discrimination rates of the proposed network is slightly lower than those of the others, which are caused by calculation errors such as exponential functions and the calculable range of the DSM. However, it was confirmed that the proposed PNN

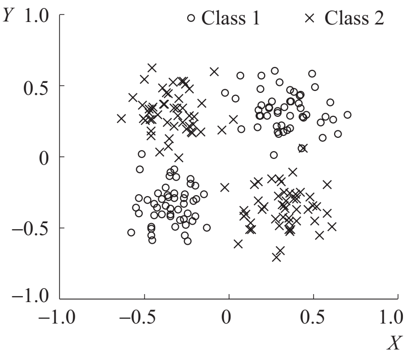

Fig. 4. Scatter graph of discrimination data.

TABLE I
COMPARISON OF THE DISCRIMINATION RATES.

	Mean [%]	S. D.
MLP	97.53	4.58×10^{-1}
$\mathrm{LLGMN_{Soft}}$	97.89	1.28×10^{-1}
$\mathrm{LLGMN_{Hard}}$[5]	97.66	1.33×10^{-1}
DSM + LLGMN	97.02	4.98×10^{-1}

exhibits high performance in pattern discrimination because the difference in the discrimination rates between the software implementation of the LLGMN and the proposed PNN is 0.87 [%].

The discrimination rates of the proposed network during a change in N in the calculation with the weight coefficients (see (7)) are shown in Fig. 5. In this figure, N is represented on the horizontal axis, and the average and standard deviations of the discrimination rates for 20 sets of the discrimination results, each of which contains 4000 samples, is shown on the vertical axis. Also, the average of the discrimination rates of the software implementation of the LLGMN is shown by the dotted line. When N is large enough, it is confirmed that the proposed network has a high accuracy of pattern discrimination at the same level as the software implementation of the LLGMN.

The digital circuit scales in the hardware implementation of the LLGMN were 982,058, and the one of the proposed network scales 961,132. As for the discrimination phase, 247 cycles were required for processing one sample in the hardware implementation of the LLGMN while 217 cycles required for the proposed network. Thus, we confirmed that the proposed network can be decreased 2.13 [%] of digital circuit scales, and the calculation speed increased 12 [%].

IV. EMG discrimination

In order to confirm the effectiveness of the pattern discrimination with bioelectric signals, EMG discrimination experiments were conducted. An EMG signal contains a lot of important information such as muscle force, intended motion of the user, and muscle impedance. If user's motion information can be discriminated based on EMGs in the hardware, these applications can be realized as practical systems such as a

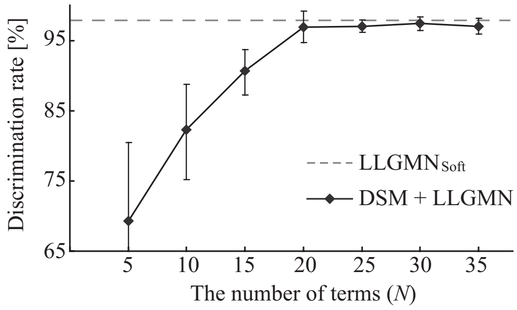

Fig. 5. Discrimination rates against the number of terms in the calculation of the weight coefficients, N.

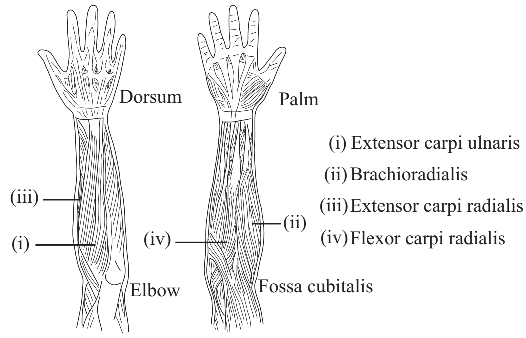

Fig. 6. Locations of electrodes.

Fig. 7. Forearm motions used in the experiments.

downsized human-machine interface system. In this section, the feature extraction method and discrimination algorithm of EMG signals are discussed.

A. Feature extraction of EMG

The contraction patterns based on the coordination of muscles can be extracted from the EMG signals measured from the user and used for pattern discrimination. First, full-wave rectification for EMG signals, $EMG_l(t)$ $(l = 1, \cdots, L)$, measured by L pairs of surface electrodes is carried out. Then, the rectified EMG signals are smoothed using a second low-pass filter, whose cut-off frequency is f_d [Hz]. The normalized signals, the sum of which for all channels makes 1, are converted into an input vector $\boldsymbol{x}(t) = [x_1(t), x_2(t), \ldots, x_L(t)]^{\mathrm{T}}$ for time t and are used for pattern discrimination. Each vector element then becomes

$$x_l(t) = \frac{EMG_l(t) - EMG_l^{st}}{\sum_{l'=1}^{L}(EMG_{l'}(t) - EMG_{l'}^{st})} \tag{9}$$

where EMG_l^{st} is the average of the $EMG_l(t)$ measured at rest. Then, the input vector $\boldsymbol{x}(t)$ is resampled at a sampling frequency f_h [Hz] after it is interpolated using the linear interpolation method since $\boldsymbol{x}(t)$ is modulated to 1-bit pulse signals using DSMs. After it is resampled in each channel as the input, the discrimination is conducted using the proposed network. Further, the user's force information for $\boldsymbol{x}(t)$ is defined as follows:

$$F_{EMG}(t) = \frac{1}{L}\sum_{l=1}^{L}\frac{EMG_l(t) - EMG_l^{st}}{EMG_l^{max} - EMG_l^{st}} \tag{10}$$

where EMG_l^{max} is the average of $EMG_l(t)$ at the maximum voluntary contraction of the muscle. By comparing $F_{EMG}(t)$ and the threshold M_d of the motion occurrence, we can determine the timing of the motion occurrence. When $F_{EMG}(t)$ exceeds M_d, the movement is estimated from the input vector $\boldsymbol{x}(t)$ using the NNs.

B. Discrimination experiments of EMG

In order to verify the validity of the proposed PNN, EMG discrimination experiments were conducted. EMG patterns were measured from five healthy subjects (A−E: male) and an upper-extremity amputee (F: male). Subject F had lost his forearm about 3 cm from the left wrist. We measured the EMG at the four locations (extensor carpi ulnaris, brachioradialis, extensor carpi radialis, and flexor carpi radialis; see Fig. 6) by using four pairs of Ag/AgCl electrodes (SEB120, GE marquette Corp., $L = 4$) with each subject. The EMG was recorded at a sampling frequency of 1 [kHz], and it was filtered by the second low-path filter (cut-off frequency: $f_d = 1$ [Hz]) after full-wave rectification. Further, the normalized EMG patterns were resampled at a resampling frequency of $f_h = 25$ [MHz]. The subject was asked to perform the following four motions ($K = 4$) continuously for five-second periods in the given order: M1: hand opening, M2: hand grasping, M3: wrist extension, and M4: wrist flexion (see Fig. 7). Also, the number of terms in the calculation with the weight coefficients (7) was $N = 30$, the order of Taylor series $C = 4$, and the number of components of the LLGMN $M_k = 2$.

An example of the measured EMG of Subject F is shown in Fig. 8. In this figure, four channels of the input EMG and the force information $F_{EMG}(t)$ are shown. We asked the subject to perform the four motions continuously. From the figure, it is shown that the EMG pattern is different for each motion. The average of the discrimination rate with 20 trials of these data was 97.62 ± 1.87 [%], where the initial weight coefficients were changed in each trial. It should be noted that the feature extraction of the EMG was implemented in the software, and the FPGA was only discriminated in terms of the EMG patterns.

The discrimination rates of the EMG measured from six subjects are shown in Fig. 9, which are represented by the software implementation of the LLGMN using C language and the proposed hardware implementation of the LLGMN using DSMs. In the experiments, we measured the EMG from each subject five times, who performed the four motions continu-

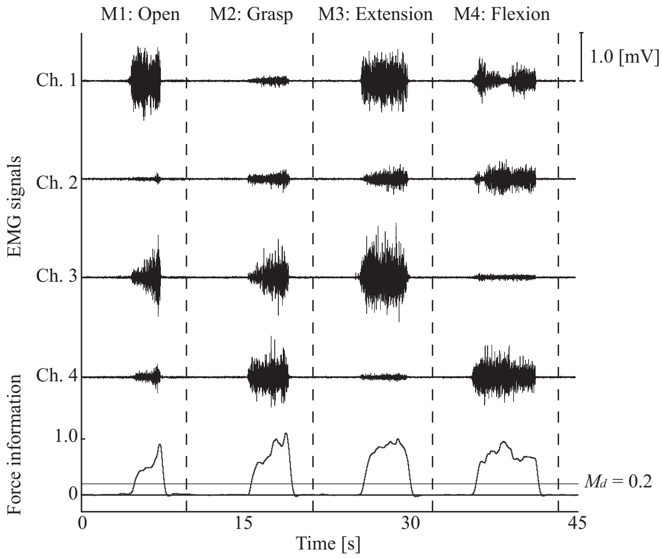

Fig. 8. Measured EMG signals of each motion (Subject F).

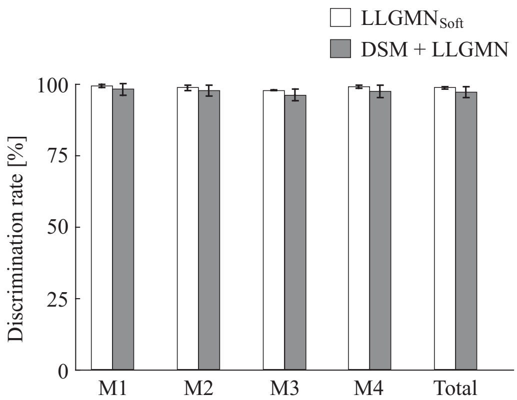

Fig. 9. Discrimination results of forearm motions with all subjects.

ously, and 20 trials were conducted with different initial weight coefficients. From this figure, we confirmed that the proposed network has a high accuracy of pattern discrimination at the same level as the software implementation of LLGMN. The discrimination rates of all the trials in the software implementation of the LLGMN and the proposed PNN were 98.52 ± 0.45 [%] and 96.98 ± 1.98 [%], respectively. Thus, it is shown that the standard deviation of the discrimination rates with the proposed network is slightly larger than those of others, which is caused by calculation errors such as the terms in the weight coefficients N. Because the difference in the discrimination rates between the software implementation of the LLGMN and the proposed PNN is only 1.54 [%], it was confirmed that the proposed PNN has a high performance in the case of pattern discrimination for EMG patterns.

V. Conclusions and Future Works

In this paper, we proposed the PNN using DS modulation for implementation in digital hardware with the aim of realizing a high accuracy of the discrimination for bioelectric signals. We confirmed that the proposed network can be decreased 2.13 [%] of digital circuit scales, and it can be increased 12 [%] of calculation speed. Further, since the discrimination rates of the proposed PNN was 96.98 ± 1.98 [%], we showed that the proposed PNN has a high performance in the case of the EMG discrimination as well.

Human-machine interface systems using EMGs, which were developed in our previous studies [4]–[7], are very useful for people with several physical disabilities. In the future, we plan to study the human-machine interface using the proposed PNN, and we intend to improve the decision algorithm of the parameters, e.g., the terms in the weight coefficients N. Furthermore, we plan to realize an on-chip learning algorithm using DS modulation on a FPGA.

Acknowledgment

This study was supported in part by a Grant-in-Aid for Scientific Research from the Research Fellowships of the Japan Society for the Promotion of Science for Young Scientists.

References

[1] D. F. Specht, "Probabilistic Neural Networks," *Neural Networks*, Vol. 3, No. 1, pp. 109–118, 1990.

[2] G. D. Zhang, "Neural Network for classification: A survey," *IEEE Transaction on Systems, Man, and Cybernetics-Part C: Applications and Reviews*, Vol. 30, No. 4, pp. 451–462, 2001.

[3] T. Tsuji, O. Fukuda, H. Ichinobe, and M. Kaneko, "A Log-Linearized Gaussian Mixture Network and Its Application to EEG Pattern Classification," *IEEE Transactions on Systems, Man, and Cybernetics-Part C: Applications and Reviews*, Vol. 29, No. 1, pp. 60–72, 1999.

[4] O. Fukuda, T. Tsuji, M. Kaneko and A. Otsuka, "A Human-Assisting Manipulator Teleoperated by EMG Signals and Arm Motions," *IEEE Transactions on Robotics and Automation*, Vol.19, No.2, pp.210–222, 2003.

[5] N. Bu, T. Hamamoto, T. Tsuji, and O. Fukuda, "FPGA Implementation of a Probabilistic Neural Network for a Bioelectric Human Interface," *The 2004 IEEE International Midwest Symposium on Circuits and Systems*, Vol. 3, pp. 29–32, 2004.

[6] K. Shima, M. Okamoto, N. Bu, and T. Tsuji, "Novel Human Interface for Game Control Using Voluntarily Generated Biological Signals," *Journal of Robotics and Mechatronics*, Vol. 18, No. 5, pp. 626–633, 2006.

[7] K. Shima, R. Eguchi, K. Shiba, and T. Tsuji, "CHRIS: Cybernetic Human-Robot Interface Systems," *Proceedings of 36th International Symposium on Robotics*, WE1C3, 2005.

[8] M. Porrmann, U. Witkowski, H. Kalte and U. Rückert, "Implementation of Artificial Neural Networks on a Reconfigurable Hardware Accelerator," *Proceedings of 10th Euromicro Workshop on Parallel, Distributed and Network-based Processing*, pp. 243–250, 2002.

[9] D. Anguita, A. Boni, and S. Ridella, "A Digital Architecture for Support Vector Machines: Theory, Algorithm, and FPGA Implementation," *IEEE Transactions on Neural Networks*, Vol. 14, No. 5, pp. 993–1009, 2003.

[10] Y. C. Kim and M. A. Shanbaltt, "Random noise effects in pulse-mode digital multilayer neural networks," *IEEE Transaction on Neural Networks*, Vol. 6, No. 1, pp. 220–229, 1995.

[11] Y. Murahashi, H. Hotta, S. Doki, and S. Okuma, "Pulsed neural networks based on delta-sigma modulation with GHA learning rule and their hardware implementation," *Systems and Computers in Japan*, Vol. 36, No. 9, pp. 14–24, 2005.

[12] T. Okuda, S. Doki, and M. Ishida, "Realization of Back Propagation Learning for Pulsed Neural Networks Based on Delta-Sigma Modulation and Its Hardware Implementation," *The IEICE Transactions on Information and Systems*, Vol. J88-D-II, No. 4, pp. 778–788, 2005 (in Japanese).

[13] C. A. Berenstein, and R. Gay, *Complex Variables. An Introduction*, Springer, pp. 104–105, 1991.